AMERICAN JOURNAL OF PHYSIOLOGY
CELL PHYSIOLOGY

Am J Physiol Cell Physiol. 2009 Apr; 296(4): C654–C662. PMCID: PMC2670652
Published online 2008 Dec 3. doi: 10.1152/ajpcell.00509.2008: 10.1152/ajpcell.00509.2008 PMID: 19052257

The Na^+/I^- symporter mediates active iodide uptake in the intestine

Juan Pablo Nicola,[1] Cécile Basquin,[1,*] Carla Portulano,[1,*] Andrea Reyna-Neyra,[2] Monika Paroder,[1] and Nancy Carrasco[1]

Departments of [1]Molecular Pharmacology and [2]Neuroscience, Albert Einstein College of Medicine, Bronx, New York
[*]C. Basquin and C. Portulano contributed equally to this work.
Address for reprint requests and other correspondence: N. Carrasco, Dept. of Molecular Pharmacology, Albert Einstein College of Medicine, 1300 Morris Park Ave., Bronx, NY 10461 (e-mail: carrasco@aecom.yu.edu)

Received 2008 Oct 8; Accepted 2008 Dec 1.

Abstract

Absorption of dietary iodide, presumably in the small intestine, is the first step in iodide (I^-) utilization. From the bloodstream, I^- is actively taken up via the Na^+/I^- symporter (NIS) in the thyroid for thyroid hormone biosynthesis and in such other tissues as lactating breast, which supplies I^- to the newborn in the milk. The molecular basis for intestinal I^- absorption is unknown. We sought to determine whether I^- is actively accumulated by enterocytes and, if so, whether this process is mediated by NIS and regulated by I^- itself. NIS expression was localized exclusively at the apical surface of rat and mouse enterocytes. In vivo intestine-to-blood transport of pertechnetate, a NIS substrate, was sensitive to the NIS inhibitor perchlorate. Brush border membrane vesicles accumulated I^- in a sodium-dependent, perchlorate-sensitive manner with kinetic parameters similar to those of thyroid cells. NIS was expressed in intestinal epithelial cell line 6, and I^- uptake in these cells was also kinetically similar to that in thyrocytes. I^- downregulated NIS protein expression and its own NIS-mediated transport both in vitro and in vivo. We conclude that NIS is functionally expressed on the apical surface of enterocytes, where it mediates active I^- accumulation. Therefore, NIS is a significant and possibly central component of the I^- absorption system in the small intestine, a system of key importance for thyroid hormone biosynthesis and thus systemic intermediary metabolism.

Keywords: dietary iodide absorption, active iodide transport, sodium/iodide symporter, enterocyte brush border

IODIDE (I^-) UPTAKE in the thyroid gland is the first step in the biosynthesis of the thyroid hormones triiodothyronine (T_3) and thyroxine (T_4), of which iodine is an essential constituent (18). T_3 and T_4 are the only iodine-containing hormones in vertebrates and are required for the development of the central nervous system and lungs in the fetus and newborn. These hormones are primary regulators of intermediary metabolism and exert pleiotropic effects in many organs and tissues. Iodine is extremely scarce in the environment and is only supplied to the body in the diet. Insufficient dietary intake of iodine, depending on its severity, causes hypothyroidism, goiter, stunted growth, retarded psychomotor development, and irreversible mental retardation (cretinism) (1, 2). Iodine deficiency disorders (IDDs) constitute the leading preventable cause of mental retardation in the world and were therefore slated by the World Health Organization for total global eradication by the year 2000 by iodination of table salt in as many countries as possible. Although significant strides have been made in many regions, as of 2007 there were still an estimated 1.9 billion people suffering from or at risk of IDDs, and IDDs are still the most common preventable cause of mental retardation (1, 2).

Active I^- accumulation in the thyroid is mediated by the Na^+/I^- symporter (NIS), a plasma membrane glycoprotein (13). Using as its driving force the Na^+ gradient generated by the Na^+-K^+-ATPase, NIS couples the inward movement of Na^+ in favor of its concentration gradient to the inward movement of I^- against its electrochemical gradient. Characteristic hallmarks of NIS are its Na^+ dependence (13, 24, 42) and its sensitivity to inhibition by perchlorate (ClO_4^-) (55). The presence of NIS in the thyroid appears to be an adaptation to compensate for the environmental scarcity of iodine. One of the most conspicuous medical applications of NIS is as the mediator of radioiodide administered to treat thyroid cancer remnants and metastases after thyroidectomy, the most effective targeted internal radiation anti-cancer therapy ever devised (39, 40).

NIS mediates I^- uptake in several tissues besides the thyroid, including lactating mammary gland, gastric mucosa, and salivary glands (9, 14, 18, 48). In all four of these tissues, NIS is located on the basolateral surface of the epithelial cells. In the lactating mammary gland, NIS activity results in the translocation of I^- from the bloodstream to the milk, thus supplying this essential anion for thyroid hormone biosynthesis by the nursing newborn (48). In both gastric mucosa and salivary glands, NIS similarly transports I^- from the bloodstream into the epithelial cells, from which I^- is released into the gastric juice (48) and saliva (12a), respectively; i.e., I^- is secreted into the gastrointestinal tract, probably via Cl^- channels (10, 18, 30). The functional significance of NIS-mediated I^- uptake in the latter two tissues is unknown. However, antioxidant and antimicrobial activities of I^- have been proposed to take place in these tissues (21, 25, 26). I^- thus released to the gastric juice and saliva is most likely reabsorbed further down the gastrointestinal tract along with newly ingested I^-. In the face of the environmental scarcity of iodine, this mechanism may contribute to the conservation and reutilization of I^-.

A key aspect of the current and future medical applications of NIS, particularly in cancer, is its status as a protein that mediates the same transport process in all tissues that express it but is regulated differently in each of these tissues (17, 51). Thus, in the healthy thyroid, NIS is expressed virtually on a continuous basis while subjected to upregulation by TSH (49) and downregulation by I^- itself (17, 22, 23, 27). In the breast, NIS is expressed only during pregnancy and lactation but

not in healthy nonlactating tissue. Remarkably, we have reported that as many as 80% of breast cancers express NIS (48, 52), as well as some breast cancer metastases (41, 51), suggesting that cell proliferation in breast cancer cells activates regulatory mechanisms that upregulate NIS. These observations may lead to the future application of radioiodide therapy to breast cancer. On the other hand, whereas NIS is constitutively expressed in the healthy stomach, we have recently shown that NIS is downregulated in gastric cancer (5). Of relevance to public health is our recent discovery that NIS actively translocates the environmental pollutant ClO_4^-. Strikingly, from a mechanistic standpoint, NIS displays different stoichiometries with different substrates (2 Na^+ per I^- and 1 Na^+ per ClO_4^-) (19).

Given the physiological significance of iodine, the question of where and how dietary I^- is absorbed in the gastrointestinal tract has long been of major interest. Reports on the absorption of I^- in the intestine appeared as early as 1912 (28). In the 1950s, some authors suggested that I^- might be both absorbed from and secreted to the intestinal lumen (3, 29, 43). Passive or simple diffusion of iodide from the intestinal lumen to the bloodstream was believed to be the mechanism in iodide absorption (16).

However, neither the existence nor the identity of a putative intestinal I^- transporter could be ascertained. No information even on the thyroid I^- transporter was available at the molecular level until 1996, when our group isolated the cDNA that encodes NIS (13). Tellingly, before its cloning, the I^- transporter was long regarded as a likely thyroid-specific protein, presumably not expressed in any other tissues. However, since NIS was identified, we and others have shown that NIS is the mediator of active I^- uptake in all tested tissues that exhibit such activity (9, 10, 47, 48). It should be emphasized that gastric NIS clearly does not mediate I^- absorption into the bloodstream, given the above mentioned location of gastric NIS at the basolateral surface of the gastric mucosa epithelial cells, which therefore translocate I^- in the opposite direction, i.e., from the bloodstream to the gastric lumen.

Here we demonstrate, for the first time, that NIS is functionally expressed in vivo on the apical surface (i.e., brush border or BB) of small intestine enterocytes in rats and mice. We also show that BB membrane vesicles (BBMV) enriched for NIS protein expression display pronounced NIS-mediated I^- uptake with kinetic characteristics very similar to those of the extensively studied rat thyroid-derived FRTL-5 cells. We additionally report that I^- downregulates its own transport in the small intestine in vivo, just as it does in the thyroid.

MATERIALS AND METHODS

Immunohistochemistry. All experimental protocols were approved by the Animal Care and Use Committee of the Albert Einstein College of Medicine. Rats and mice were anesthetized and their abdomens were opened. The small intestine was perfused with 10% neutral buffered formalin (NBF) before or right after resection from the animal and cut in approximately 8-cm fragments, and each fragment was filled with 10% NBF, ligated at both ends, and fixed overnight in 10% NBF. Paraffin-embedded blocks were prepared containing longitudinal and cross-sectional intestinal segments. Tissue sections (5-μm) made from the paraffin blocks were deparaffinated. Antigen retrieval was performed by incubation with boiling 10 mM citrate buffer (pH 6.0) for 15 min.

Endogenous peroxidase activity was quenched for 10 min with 3% H_2O_2 in methanol, and tissue sections were blocked for 1 h with 5% goat serum in PBS. After 30 min of incubation with (or without, for negative controls) 6.7 nM affinity-purified rabbit anti-NIS antibody (35) diluted in 0.5% BSA in PBS, slides were incubated for 10 min with anti-rabbit poly-horseradish peroxidase-conjugated antibody (SuperPicture, Zymed Laboratories). The chromogen solution was applied for 3 to 7 min until the peroxidase reaction took place. Tissue sections were counterstained, dehydrated, mounted, and dried overnight.

Cell culture. FRTL-5 cells derived from Fisher rat thyroids were cultured as previously described (46). Epithelial cell line 6 (IEC-6) cells derived from rat normal small intestine epithelium were purchased from American Type Culture Collection (Manassas, VA) and cultured in Dulbecco's modified Eagle's medium adjusted to contain 3.7 g/l sodium bicarbonate, 4 mM L-glutamine, and supplemented with 0.1 U/ml bovine insulin and 5% calf bovine serum. IEC-6 cells expressed NIS after *passage 36*.

RNA isolation and RT-PCR. Total RNA was purified from isolated enterocytes by the acid guanidinium thiocyanate/phenol/chloroform extraction procedure as previously described (12). cDNA was synthesized from 2 μg of total RNA. PCR was performed in a 20-μl reaction volume containing 2 μl cDNA reaction, 0.5 μM of each primer, 0.25 mM of each dNTP, 1.5 mM $MgCl_2$, and 1 unit Taq polymerase. Samples were heated to 95°C for 5 min and then subjected to 36 cycles of amplification for NIS and 28 cycles for β-actin, performed as follows: denaturation at 95°C for 30 s, annealing at 59°C for 30 s, and extension at 72°C for 30 s, followed by a 7-min extension at 72°C after the last cycle. Primers for the rat NIS gene were 5′-GCTGTGGCATTGTCATGTTC (forward) and 5′-TGAGGTCTTCCACAGTCACA (reverse). The amplification yielded a 219-bp DNA product whose sequence corresponded to bp 1002–1220 of the rat NIS cDNA (13). Primer oligonucleotides for rat β-actin were 5′-CGACGAGGCCCAGAGCAAGAGAGG (forward) and 5′-CGTCAGGCAGCTCATAGCTCTTCTCCAGGG (reverse). The amplification yielded a 568-bp DNA product corresponding to bp 246–814 of rat β-actin cDNA. The expression of β-actin was used as loading control. Primers for the amplification were 5′- CTGCTGAGCAGGAATCCACA (forward) and 5′-TAGTTGACATCACCACTCTC (reverse) for the alkaline phosphatase (ALP), and 5′-TACTCTGCGCTCCGAAGGCT (forward) and 5′-CTGTAGGAGACAGTGGAGTG for PCNA. The amplifications yielded a 364-bp and a 523-bp DNA product, whose sequences corresponded to bp 996 to 1360 and 212 to 735, respectively, of the rat sequences. The amplification of all products remained within the exponential range. Reaction conditions were optimized by assessing the variation in signal intensity at different sample amounts and cycle numbers. Genomic DNA contamination was excluded, because extra bands were not observed even though the primer pairs used for NIS and β-actin spanned introns. As a positive control, the same amount of total RNA from FRTL-5 cells was used, and as negative controls, reactions without reverse transcription or PCR without cDNA were carried out in parallel. PCR products were separated on 1.5% agarose gel and visualized with ethidium bromide.

In vivo intestinal uptake. Adult male Sprague-Dawley rats (300–320 g) were food deprived overnight, and the next day, rats were laparotomized and the stomach and duodenum were exposed. A 2-mm puncture wound was made in the duodenal wall with a 22-gauge needle, and a Silastic tube (0.25 mm ID, 0.063 mm OD) for duodenal infusions was advanced 1 cm and fixed us-

ing a monofilament knitted polypropylene mesh (Bard, Murray Hill, NJ). An internal jugular vein catheter was placed in the right atrium for blood sampling. The jugular catheter was kept permeable with an infusion of heparinized saline (50 IU) (0.2 ml). Both catheters were routed subcutaneously to the back of the neck and secured to an infusion button. When not in use, both catheters were closed with stainless steel blockers. Pertechnetate ($^{99m}TcO_4^-$) (Cardinal Health) (500–800 μCi) was administered through the duodenal catheter, followed by saline solution (200 μl). Blood was collected through the jugular catheter 9 min after $^{99m}TcO_4^-$ administration. Aliquots from each blood sample (10 μl) were measured in duplicate using a γ-counter. After 2 h, the same animals were given the same amount of $^{99m}TcO_4^-$ supplemented with $NaClO_4$ (100–580 nmol), and blood samples were collected and measured as described above. Data are expressed as percentage of the administered dose per milliliter of blood.

Preparation of BBMV. Intestinal cells were isolated according to Weiser's method (53). Briefly, rat small intestine was washed three times with a physiological solution containing 0.154 M NaCl and 1 mM DTT. To isolate villus-tip epithelial cells, excluding cryptic epithelial, serosal, and interstitial cells, the intestine was filled with a solution containing 1.5 mM KCl, 96 mM NaCl, 27 mM sodium citrate, 8 mM KH_2PO_4, and 5.6 mM Na_2HPO_4 (pH 7.3) for 10 min to dissociate cells. The intestine was treated with PBS containing 1.5 mM EDTA and 0.5 mM DTT for 15 min, and released cells were collected. Villus-tip epithelial cells were washed twice with PBS and placed in ice-cold sucrose buffer [250 mM sucrose, 2 mM Tris·HCl (pH 7.4), and protease inhibitors]. Resuspended cells were homogenized using a polytron homogenizer (four 30-s pulses) and centrifuged at 3,000 *g* for 10 min. The resulting turbid supernatant (*fraction A*) was centrifuged at 20,500 *g* for 20 min at 4°C. The lower brown pellet (*fraction B*) was resuspended in sucrose buffer and subjected to glass-Teflon homogenization. $CaCl_2$ was added to the homogenates, reaching a final concentration of 10 mM. This mixture was incubated for 20 min on ice to allow preferential precipitation of non-BB components. The precipitated material was pelleted by centrifugation at 3,000 *g* for 10 min. The supernatant was decanted and centrifuged again for 20 min at 20,500 *g*. The resulting pellet (*fraction C*) was resuspended in sucrose buffer containing 10 mM $CaCl_2$ and centrifuged at 48,000 *g* for 30 min to obtain the final BBMV pellet. Membrane vesicles were resuspended in 250 mM sucrose, 1 mM $MgCl_2$, 10 mM HEPES (pH 7.4), and protease inhibitors (36).

Where indicated, BBMV were also prepared from four different groups of Sprague-Dawley rats (two to four animals per group) with different I^- intake exposures: a control (nontreated) group and groups that were administered autoclaved tap water supplemented with 0.05% KI for 12 h, 24 h, or 48 h (22). Water was changed every day. Food was made available ad libitum.

Internal volume of BBMV. BBMV intravesicular volume was quantitated by a modification of the method described by Kaminsky et al. (31). Aliquots containing BBMV (100 μg) were incubated for 12 h at 4°C with an equal volume of assay solution, as described in BBMV I^- uptake assays, but containing choline chloride (200 mM) instead of NaCl, and different concentrations of $^{125}I^-$ (20 and 100 μM). Under these conditions, only passive diffusion takes place. Reactions were terminated by rapid dilution and filtration. The internal volume was calculated from $^{125}I^-$ equilibration values.

ALP activity. ALP activity was determined with a kinetic modification of a technique previously described (7). Briefly, 20 μg of protein was incubated in 1 M diethanolamine buffer (pH 9.8), 0.5 mM $MgCl_2$, and 10 mM *p*-nitrophenylphosphate substrate at 37°C. The amount of released *p*-nitrophenol product was measured by determining the absorbance at 405 nm. Each protein sample was measured in triplicate. Enzyme activity was expressed in IU/mg protein.

Immunoblot analysis. Total protein extracts or membrane fractions were immunoblotted as described previously (15), except that 2.2 nM affinity-purified anti-rat NIS antibody was used (35). Loading controls were performed with monoclonal antibodies against α-tubulin (1:4,000 dilution; Sigma) and E-cadherin antibody (1:5,000 dilution; BD Transduction) or anti-ezrin polyclonal antibody (1:500 dilution; Santa Cruz).

I^- transport. I^- transport assays in intact cells were carried out as previously described (15). Steady-state uptake experiments (40 min at 37°C) were performed with 20 μM NaI supplemented with carrier-free $Na^{125}I$ to give a specific activity of 100 mCi/mmol. For initial-rate (2 min) I^- transport assays, KI at various concentrations was used. For standardization, DNA was determined by the diphenylamine method after trichloroacetic acid precipitation, and uptake was expressed as pmol I^-/μg DNA.

I^- uptake in BBMV was carried out as described previously (15), except that 20 μM NaI supplemented with $^{125}I^-$ to reach a specific radioactivity of 100 mCi/mmol and 0.45-μm-pore-diameter nitrocellulose filters were used. To assess Na^+ dependence, incubations were done in final 100 mM choline chloride instead of NaCl to maintain isotonicity. ClO_4^- inhibition was tested by adding 40 μM $KClO_4$ to the incubation buffer. Reactions were terminated as described previously (15) after 5 s for initial-rate assays and 5 min for steady-state assays and after the indicated time points for the time course, and membranes were washed twice with additional 3-ml ice-cold quenching solution. Radioactivity retained in BBMV was determined by measuring filters in a γ-counter. Data, in duplicate, were standardized per amount of protein and expressed as pmol $^{125}I^-$/mg protein.

Immunofluorescence analysis. IEC-6 cells were seeded onto coverslips. After 24 h, cells were washed thrice in PBS containing 0.1 mM $CaCl_2$ and 1 mM $MgCl_2$ (PBS-CM), fixed with 2% paraformaldehyde for 15 min at room temperature, and quenched three times for 10 min each time with PBS supplemented with 100 mM glycine. Cells were permeabilized with PBS-CM-0.1% Triton X-100 for 5 min, rinsed twice for 10 min each time with PBS-CM-0.1% BSA, and incubated for 1 h at room temperature with 4 nM affinity-purified rabbit anti-NIS antibody and mouse anti-α_1-subunit of the Na^+-K^+-ATPase antibody 1:700 (Upstate Biotechnology) in PBS-0.1% BSA. Cells were washed three times for 10 min with PBS, incubated for 1 h in the dark with anti-rabbit Alexa-488 and anti-mouse Alexa-594 secondary antibodies (Molecular Probes) (1:350 dilution), and washed as above. Coverslips were mounted onto slides with Slow Fade antifade reagent (Molecular Probes). Cells were visualized in a Bio-Rad Radiance 2000 Laser Scanning Confocal Microscope (Bio-Rad Laboratories).

RESULTS

NIS is expressed on the apical surface of small intestine enterocytes. We analyzed paraffin-embedded sections of small intestine from rats and mice by immunohistochemistry with anti-NIS antibody, as described in MATERIALS AND METHODS. NIS expression was clearly apparent along the entire length of the small intestine exclusively on the apical surface of the enterocytes (Fig. 1, *A–F*), a finding compatible with the notion that NIS may translocate I^- from the intestinal lumen into these cells, from which I^- would efflux basolaterally toward the bloodstream. No staining was observed when only the second antibody was used (data not shown). To investigate at the functional level whether the absorption of I^- is mediated by NIS in vivo, we administered pertechnetate ($^{99m}TcO_4^-$) [a widely used NIS substrate with a shorter half-life than $^{125}I^-$ (48)] alone and, after a 2-h washout time, $^{99m}TcO_4^-$ together with the NIS inhibitor ClO_4^- to four rats via duodenal catheterization, and collected blood samples. Nine minutes after administration, the absorption of $^{99m}TcO_4^-$ in the animals simultaneously treated with ClO_4^- was inhibited by 27.4% to 47.9% as compared with those treated with $^{99m}TcO_4^-$ alone (Fig. 1*G*).

To assess our initial observation that NIS is more abundantly expressed toward the tip of the villus, we isolated nine fractions of epithelial cells, from the villus tip to the crypt, following the protocol described by Weiser (53). NIS mRNA (standardized relative to β-actin mRNA expression) was clearly enriched (~5- to 6-fold) in cells from the tip of the villus (Fig. 2*A*, *fractions 1* and *2*), decreasing as cells approached the crypt (Fig. 2*A*, *fractions 5-9*). NIS mRNA distribution followed that of intestinal ALP mRNA, a marker that is more abundant at the villus tip (53), in contrast to the distribution of PCNA mRNA, which decreases toward the tip of the villus (38). Given the predominant apical expression of NIS, we isolated villus-tip cells and purified BB membranes enriched for membrane proteins. As expected, there was a pronounced enrichment in ALP activity (~20-fold) in membranes over cell homogenates (Fig. 2*B*). At the same time, immunoblot analysis of these enriched BB membranes from enterocytes revealed an ~90-kDa polypeptide (Fig. 2*C*, *fraction C*) corresponding to intestinal NIS, whose electrophoretic mobility was identical to that of NIS from the rat thyroid-derived FRTL-5 cells. NIS was undetectable in intestinal cell homogenates (*fraction A*) and became apparent in the partially purified *fraction B* (Fig. 2*C*). Protein loading controls using anti-ezrin antibody are shown at the bottom of Fig. 2*C*.

BBMV display pronounced NIS-mediated I^- uptake. To further assess the functional significance of NIS expression in enterocyte BB, we prepared sealed BBMV and performed steady-state I^- transport assays (Fig. 3*A*) after determining that saturation was reached at 5 min (Fig. 3*A*, *inset*). BBMV took up as much as 120 pmol I^-/mg protein, and transport was both Na^+ dependent and ClO_4^- inhibitable. Na^+ dependence was tested by using choline chloride instead of Na^+, thus maintaining the osmolarity constant. BBMV initial-rate I^- transport (carried out at 5-s time points) showed a K_m for I^- of 13.4 ± 2.0 μM, a value comparable to those reported for thyroid membrane vesicles (42), and was inhibited by ClO_4^- (Fig. 3*B*). In addition, we demonstrated that NIS-mediated I^- uptake in these BBMV is active transport (i.e., it occurs against an I^- concentration gradient) by determining that the intravesicular volume was 1.7 μl/mg protein and the calculated I^- concentration gradient was as large as fivefold.

IEC-6 cells exhibit NIS-mediated I^- uptake. IEC-6 cells derive from the entire small intestine of newborn rats (45). We assessed NIS expression in these cells by subjecting IEC-6 cell lysates to immunoblot analysis (Fig. 4*A*). NIS expression in IEC-6 cells was actually slightly higher than in rat

thyroid-derived FRTL-5 cells. Given that NIS must be in the plasma membrane for I^- uptake to take place, we performed confocal immunofluorescence studies in IEC-6 cells, which displayed a characteristic NIS plasma membrane-associated immunofluorescence staining pattern (Fig. 4*B*, *top*), which overlaps with that of the Na^+-K^+-ATPase α-subunit, a plasma membrane marker (Fig. 4*B*, *middle* and *bottom*). This overlap occurs because the IEC-6 cells were grown on plastic, where there is no differentiation between the basolateral and apical compartments.

We carried out steady-state I^- transport assays in IEC-6 cells. These cells accumulated ~90 pmol I^-/μg DNA, as compared with 55 pmol I^-/μg DNA for FRTL-5 cells; i.e., ClO_4^--inhibitable active I^- uptake was observed at levels even higher than those in FRTL-5 cells (Fig. 4*C*), a result consistent with the above mentioned NIS expression findings.

We then analyzed the kinetic properties of NIS activity in IEC-6 cells as compared with those of NIS in control FRTL-5 cells. Initial I^- uptake rates (2-min time points) were assessed by measuring I^- accumulation at varying I^- concentrations ranging from 0 to 160 μM at a constant Na^+ concentration (140 mM) (Fig. 4*D*). Intestinal NIS exhibited a similar K_m value ($K_{m\ I-}$ = 20.3 ± 3.9 μM) but a significantly higher maximal transport rate ($V_{max\ I-}$ = 99.3 ± 5.4 pmol/2 min/μg DNA) for I^- than thyroid NIS ($K_{m\ I-}$ = 13.2 ± 3.7 μM; $V_{max\ I-}$ = 32.6 ± 2.8 pmol·2 min^{-1}·μg DNA^{-1}). We observed a direct correlation between the higher IEC-6 V_{max} values (Fig. 4*D*) and the corresponding higher NIS protein expression level in IEC-6 cells relative to FRTL-5 cells (Fig. 4*A*).

I^- downregulates its own transport in intestinal NIS. I^- at saturating concentration is known to be a significant downregulator of the thyroid gland and inhibits the production of thyroid hormones. This inhibitory effect, called the Wolff-Chaikoff effect, has been reported in FRTL-5 cells and rat thyroid glands in vivo and has been shown to lead to the downregulation of NIS function and expression (17, 22, 23, 27). Here we investigated whether the anion also had a regulatory effect on NIS in rat intestine. Rats were divided into four groups (four animals per group), three of which were treated with 0.05% KI in the drinking water for 12, 24, and 48,h; the effect of I^- administration was compared with the fourth group of animals, which received only distilled water with no addition of I^-. BBMV from treated and nontreated rats were purified and used for steady-state I^- uptake assays in the absence (Fig. 5*A*, gray bars) or presence (Fig. 5*A*, black bars) of ClO_4^-. We observed that high concentrations of I^- inhibited its own NIS-mediated uptake and that the decrease in I^- transport became more pronounced with longer exposure times (Fig. 5*A*). Immunoblot analyses were carried out in BBMV obtained from each animal, and the NIS protein levels (Fig. 5*B*, *top*) were quantified by densitometry and standardized with the ezrin signal (Fig. 5*B*, *bottom*). As shown in Fig. 5, *B* and *C*, after 12 h of high I^- supplementation, NIS protein levels decreased by 48.6% with respect to the levels of the control group. After 24 and 48 h, NIS protein levels decreased by as much as 83%. Thus, our data show, for the first time, that high I^- concentrations inhibit NIS-mediated I^- uptake in vivo not only in the thyroid but also in at least one extrathyroidal tissue, i.e., the small intestine.

DISCUSSION

That I^- is likely to be absorbed in the small intestine has long been expected, even though the precise molecular mechanism by which this process occurs has not been elucidated. Shortly after the cloning of NIS in our laboratory (13), Ajjan et al. (4) reported low levels of NIS mRNA expression —by hybridizing the amplified PCR product with radiolabeled oligonucleotides—in rat small intestine, and Perron et al. (44) observed, by semiquantitative RT-PCR, levels of NIS mRNA in mouse intestine that were 4% of those observed in mouse thyroid, suggesting that NIS might play a role in I^- transport in the small intestine. However, the presence of the NIS transcript does not yet prove that the NIS protein is biosynthesized, targeted to the plasma membrane, and fully functional. In fact, reports using immunohistochemistry suggested that the NIS protein was not expressed in the intestine (34, 50), a contention we disproved when we investigated NIS protein expression in microarrays containing samples from normal human small intestine and found weak expression in two out of three samples (52). Our observations provided more persuasive but not quite conclusive evidence that NIS may be involved in I^- absorption in the small intestine, because neither NIS subcellular localization nor function was analyzed. Studies in tissue microarrays are optimal for high-throughput screening but intrinsically limited on account of the size of the samples and tissue preservation conditions. Very recently, Donowitz et al. (20) described in detail the proteome of the mouse jejunal BBMV, in which they demonstrated the presence of NIS by immunoblot and immunofluorescence as one of several validated BB proteins. We have now carried out an extensive and detailed study on NIS protein expression and activity in the rodent small intestine. We found very robust NIS expression in the BB in all segments of the small intestine, from the duodenum to the ileum, in both rats and mice, as revealed by immunohistochemistry (Fig. 1). The staining pattern was clearly apical, consistent with the proposition that NIS may mediate active I^- transport from the intestinal lumen to the cell, subsequently reaching the bloodstream, probably through Cl^- channels. In contrast, basolateral NIS-mediated I^- uptake in the thyroid, lactating breast, salivary glands, and stomach is from the bloodstream to the cell and ultimately to the colloid, milk, saliva, and gastric juice, respectively.

Our findings suggest that NIS protein expression in the intestine, as ascertained by immunohistochemistry, may have been missed by other investigators if the tissue was not optimally preserved. Regarding detection of the NIS protein in the intestine by immunoblot analysis, it clearly requires that the samples be highly enriched for BB membrane proteins. Without such enrichment, no NIS expression is detected (Fig. 2*C*, *fraction A*). In rat intestine in vivo, $^{99m}TcO_4^-$, a well-known NIS substrate, is transported into the blood very rapidly, because it could be detected in the blood as soon as 10 s after duodenal administration (data not shown). We have also observed ClO_4^--inhibitable $^{99m}TcO_4^-$ transport in vivo at later time points (Fig. 1*G*). To carry out a kinetic analysis, we studied NIS-mediated active I^- uptake in sealed BBMV (Fig. 3), a system that has been widely used to study intestinal uptake, either passive or active, of carbohydrates, amino acids, and other nutrients (6, 32, 33). The kinetic parameters of I^- transport in BBMV were comparable to those reported for FRTL-5 cells/thyroid membrane vesicles (Fig. 4*D*) (42, 54).

In addition, we have detected NIS expression and NIS activity in late-passage (*passage 37*) IEC-6 cells (Fig. 4). Whereas it is unknown why NIS expression is detected in late- but not early-passage IEC-6 cells, similar observations regarding other proteins have been made in other intestinal cells,

such as Caco-2 cells, in which the activity of the BB-associated hydrolase sucrase-isomaltase increased sevenfold from early to late passages (11); similarly, expression of the fructose transporter GLUT-5 was reported to be 10 times higher in late- as compared with early-passage Caco-2 cells (37).

Finally and significantly, we have demonstrated that I^- at high concentrations acts as a downregulator of its own NIS-mediated transport in the small intestine in vivo (Fig. 5), the first time that this autoregulatory mechanism has been observed outside the thyroid.

The extensive investigation of thyroid NIS stands in stark contrast with the extremely limited analysis of intestinal NIS performed thus far. Early studies of I^- transport in the small intestine, carried out long before NIS was identified, indicate that the anion is not only absorbed from but also secreted to the lumen (3, 29, 43). As a net absorption of dietary I^- must necessarily occur, such reports suggest that the overall handling of I^- in the gastrointestinal tract is fairly complex and may involve several different mechanisms and transport proteins. That NIS is targeted to the apical surface of enterocytes, in contrast to the basolateral targeting of NIS in most other epithelial cells that express it, affords a unique opportunity to undertake a future study of what protein-protein interactions or other factors are involved in NIS polarized targeting.

The research presented here provides strong evidence that NIS is a significant and possibly central component of the I^- absorption system in the small intestine. However, our data do not rule out the possible participation of transporters other than NIS, such as anion exchangers, in the translocation of I^- from the intestinal lumen into the enterocytes, a notion consistent with the observed partial inhibition of $^{99m}TcO_4^-$ absorption by ClO_4^-.

NIS may be thought of as a kind of I^- metabolism master molecule, participating in the anion's translocation from its intestinal absorption to its uptake in the thyroid, lactating breast, salivary glands, and gastric mucosa. In these last two tissues, NIS activity causes I^- to return to the gastrointestinal lumen, from which the anion, as part of an I^- conservation system, is again absorbed via NIS in the small intestine. Finally, in light of our recent demonstration that NIS mediates active transport of ClO_4^- (19), intestinal NIS is clearly a conduit for this environmental pollutant to enter the bloodstream.

NOTE ADDED IN PROOF

In the Articles in PresS version of this manuscript, Figs. 2*B* and 5*B* contained some errors. It was also not made explicit that the images in these panels were derived from more than one gel. The corrected versions of the figures and legends are provided here, in this final-published version.

GRANTS

This work was supported by National Institutes of Health Grants DK-41544 and CA-098390 (to N. Carrasco).

Supplementary Material

[Corrigendum]

Acknowledgments

We thank Dr. Viktoriya Paroder for initial work on IEC-6 cells. We thank Drs. Gary Schwartz and Zhiping Wu for useful advice. We are grateful to the members of the Carrasco laboratory for critical reading of the manuscript.

Present address for J. P. Nicola: Departamento de Bioquímica Clínica, Universidad Nacional de Córdoba, Córdoba, 5000 Córdoba, Argentina.

Notes

The costs of publication of this article were defrayed in part by the payment of page charges. The article must therefore be hereby marked "*advertisement*" in accordance with 18 U.S.C. Section 1734 solely to indicate this fact.

REFERENCES

1. Assessment of iodine deficiency disorders, and monitoring their elimination. Geneva, Switzerland: World Health Organization, 2007.

2. Turning the tide of malnutrition, responding to the challenge of the 21st century. Geneva, Switzerland: World Health Organization, 2002.

3. Acland JD, Illman O. Studies on iodide transport against a concentration gradient by the small intestine of the rat in vitro. *J Physiol* 147: 260–268, 1959. [PMCID: PMC1357026] [PubMed: 13791672]

4. Ajjan RA, Kamaruddin NA, Crisp M, Watson PF, Ludgate M, Weetman AP. Regulation and tissue distribution of the human sodium iodide symporter gene. *Clin Endocrinol (Oxf)* 49: 517–523, 1998. [PubMed: 9876351]

5. Altorjay A, Dohan O, Szilagyi A, Paroder M, Wapnir IL, Carrasco N. Expression of the Na^+/I^- symporter (NIS) is markedly decreased or absent in gastric cancer and intestinal metaplastic mucosa of Barrett esophagus. *BMC Cancer* 7: 5, 2007. [PMCID: PMC1794416] [PubMed: 17214887]

6. Berner W, Kinne R, Murer H. Phosphate transport into brush-border membrane vesicles isolated from rat small intestine. *Biochem J* 160: 467–474, 1976. [PMCID: PMC1164262] [PubMed: 13784]

7. Bessey OA, Lowry OH, Brock MJ. A method for the rapid determination of alkaline phosphatase with five cubic millimeters of serum. *J Biol Chem* 164: 321–329, 1946. [PubMed: 20989492]

9. Brown-Grant K Extrathyroidal iodide concentrating mechanisms. *Physiol Rev* 41: 189–213, 1961.

10. Bruno R, Giannasio P, Ronga G, Baudin E, Travagli JP, Russo D, Filetti S, Schlumberger M. Sodium iodide symporter expression and radioiodine distribution in extrathyroidal tissues. *J Endocrinol Invest* 27: 1010–1014, 2004. [PubMed: 15754731]

11. Chantret I, Rodolosse A, Barbat A, Dussaulx E, Brot-Laroche E, Zweibaum A, Rousset M. Differential expression of sucrase-isomaltase in clones isolated from early and late passages of the cell line Caco-2: evidence for glucose-dependent negative regulation. *J Cell Sci* 107: 213–225, 1994. [PubMed: 8175910]

12. Chomczynski P, Sacchi N. Single-step method of RNA isolation by acid guanidinium thiocyanate-phenol-chloroform extraction. *Anal Biochem* 162: 156–159, 1987. [PubMed: 2440339]

12a. Cohen B, Myant NB. Concentration of salivary iodide : a comparative study. *J Physiol* 145: 595–610, 1959. [PMCID: PMC1356965] [PubMed: 13642324]

13. Dai G, Levy O, Carrasco N. Cloning and characterization of the thyroid iodide transporter. *Nature* 379: 458–460, 1996. [PubMed: 8559252]

14. De La Vieja A, Dohan O, Levy O, Carrasco N. Molecular analysis of the sodium/iodide symporter: impact on thyroid and extrathyroid pathophysiology. *Physiol Rev* 80: 1083–1105, 2000. [PubMed: 10893432]

15. De la Vieja A, Ginter CS, Carrasco N. Molecular analysis of a congenital iodide transport defect: G543E impairs maturation and trafficking of the Na^+/I^- symporter. *Mol Endocrinol* 19: 2847–2858, 2005. [PubMed: 15976004]

16. Derblom H, Johansson H, Nylander G. Small intestinal absorption and gastric secretion of iodide in total small bowel obstruction in the rat. *Surgery* 54: 771–783, 1963. [PubMed: 14083588]

17. Dohan O, De la Vieja A, Carrasco N. Hydrocortisone and purinergic signaling stimulate sodium/iodide symporter (NIS)-mediated iodide transport in breast cancer cells. *Mol Endocrinol* 20: 1121–1137, 2006. [PubMed: 16439463]

18. Dohan O, De la Vieja A, Paroder V, Riedel C, Artani M, Reed M, Ginter CS, Carrasco N. The sodium/iodide symporter (NIS): characterization, regulation, and medical significance. *Endocr Rev* 24: 48–77, 2003. [PubMed: 12588808]

19. Dohan O, Portulano C, Basquin C, Reyna-Neyra A, Amzel LM, Carrasco N. The Na^+/I symporter (NIS) mediates electroneutral active transport of the environmental pollutant perchlorate. *Proc Natl Acad Sci USA* 104: 20250–20255, 2007. [PMCID: PMC2154417] [PubMed: 18077370]

20. Donowitz M, Singh S, Salahuddin FF, Hogema BM, Chen Y, Gucek M, Cole RN, Ham A, Zachos NC, Kovbasnjuk O, Lapierre LA, Broere N, Goldenring J, deJonge H, Li X. Proteome of murine jejunal brush border membrane vesicles. *J Proteome Res* 6: 4068–4079, 2007. [PubMed: 17845021]

21. El Hassani RA, Benfares N, Caillou B, Talbot M, Sabourin JC, Belotte V, Morand S, Gnidehou S, Agnandji D, Ohayon R, Kaniewski J, Noel-Hudson MS, Bidart JM, Schlumberger M, Virion A, Dupuy C. Dual oxidase2 is expressed all along the digestive tract. *Am J Physiol Gastrointest Liver Physiol* 288: G933–G942, 2005. [PubMed: 15591162]

22. Eng PH, Cardona GR, Fang SL, Previti M, Alex S, Carrasco N, Chin WW, Braverman LE. Escape from the acute Wolff-Chaikoff effect is associated with a decrease in thyroid sodium/iodide symporter messenger ribonucleic acid and protein. *Endocrinology* 140: 3404–3410, 1999. [PubMed: 10433193]

23. Eng PH, Cardona GR, Previti MC, Chin WW, Braverman LE. Regulation of the sodium iodide symporter by iodide in FRTL-5 cells. *Eur J Endocrinol* 144: 139–144, 2001. [PubMed: 11182750]

24. Eskandari S, Loo DD, Dai G, Levy O, Wright EM, Carrasco N. Thyroid Na^+/I symporter. Mechanism, stoichiometry, specificity. *J Biol Chem* 272: 27230–27238, 1997. [PubMed: 9341168]

25. Fite A, Dykhuizen R, Litterick A, Golden M, Leifert C. Effects of ascorbic acid, glutathione, thiocyanate, and iodide on antimicrobial activity of acidified nitrite. *Antimicrob Agents Chemother* 48: 655–658, 2004. [PMCID: PMC321511] [PubMed: 14742231]

26. Geiszt M, Witta J, Baffi J, Lekstrom K, Leto TL. Dual oxidases represent novel hydrogen peroxide sources supporting mucosal surface host defense. *FASEB J* 17: 1502–1504, 2003. [PubMed: 12824283]

27. Grollman EF, Smolar A, Ommaya A, Tombaccini D, Santisteban P. Iodine suppression of iodide uptake in FRTL-5 thyroid cells. *Endocrinology* 118: 2477–2482, 1986. [PubMed: 3009160]

28. Hanzlik PJ Quantitative studies on the gastro-intestinal absorption of drugs: II. The absorption of sodium iodide. *J Pharmacol Exp Ther* 3: 387–421, 1912.

29. Ilundain A, Larralde J, Toval M. Iodide transport in rat small intestine: dependence on calcium. *J Physiol* 393: 19–27, 1987. [PMCID: PMC1192377] [PubMed: 3446797]

30. Josefsson M, Evilevitch L, Westrom B, Grunditz T, Ekblad E. Sodium-iodide symporter mediates iodide secretion in rat gastric mucosa in vitro. *Exp Biol Med (Maywood)* 231: 277–281, 2006. [PubMed: 16514173]

31. Kaminsky SM, Levy O, Salvador C, Dai G, Carrasco N. Na(+)-I^- symport activity is present in membrane vesicles from thyrotropin-deprived non-$I(^-)$-transporting cultured thyroid cells. *Proc Natl Acad Sci USA* 91: 3789–3793, 1994. [PMCID: PMC43667] [PubMed: 8170988]

32. Kaunitz JD, Wright EM. Kinetics of sodium d-glucose cotransport in bovine intestinal brush border vesicles. *J Membr Biol* 79: 41–51, 1984. [PubMed: 6737463]

33. Kessler M, Tannenbaum V, Tannenbaum C. A simple apparatus for performing short-time (1–2 seconds) uptake measurements in small volumes; its application to d-glucose transport studies in brush border vesicles from rabbit jejunum and ileum. *Biochim Biophys Acta* 509: 348–359, 1978. [PubMed: 656416]

34. Lacroix L, Mian C, Caillou B, Talbot M, Filetti S, Schlumberger M, Bidart JM. Na(+)/I(-) symporter and Pendred syndrome gene and protein expressions in human extra-thyroidal tissues. *Eur J Endocrinol* 144: 297–302, 2001. [PubMed: 11248751]

35. Levy O, Dai G, Riedel C, Ginter CS, Paul EM, Lebowitz AN, Carrasco N. Characterization of the thyroid Na^+/I^- symporter with an anti-COOH terminus antibody. *Proc Natl Acad Sci USA* 94: 5568–5573, 1997. [PMCID: PMC20819] [PubMed: 9159113]

36. Maenz DD, Cheeseman CI. Effect of hyperglycemia on d-glucose transport across the brush-border and basolateral membrane of rat small intestine. *Biochim Biophys Acta* 860: 277–285, 1986. [PubMed: 3741853]

37. Mahraoui L, Rousset M, Dussaulx E, Darmoul D, Zweibaum A, Brot-Laroche E. Expression and localization of GLUT-5 in Caco-2 cells, human small intestine, and colon. *Am J Physiol Gastrointest Liver Physiol* 263: G312–G318, 1992. [PubMed: 1384349]

38. Mariadason JM, Nicholas C, L'Italien KE, Zhuang M, Smartt HJ, Heerdt BG, Yang W, Corner GA, Wilson AJ, Klampfer L, Arango D, Augenlicht LH. Gene expression profiling of intestinal epithelial cell maturation along the crypt-villus axis. *Gastroenterology* 128: 1081–1088, 2005. [PubMed: 15825089]

39. Mazzaferri EL Long-term outcome of patients with differentiated thyroid carcinoma: effect of therapy. *Endocr Pract* 6: 469–476, 2000. [PubMed: 11155222]

40. Mazzaferri EL Thyroid diseases: tumors. Radioiodine and other treatment and outcomes. In: *Werner & Ingbar's The Thyroid: A Fundamental and Clinical Text* (8th ed.), edited by Braverman LE and Utiger RD. Philadelphia, PA: Lipincott Williams & Wilkins, 2000, p. 904–930.

41. Moon DH, Lee SJ, Park KY, Park KK, Ahn SH, Pai MS, Chang H, Lee HK, Ahn IM. Correlation between ^{99m}Tc-pertechnetate uptakes and expressions of human sodium iodide symporter gene in breast tumor tissues. *Nucl Med Biol* 28: 829–834, 2001. [PubMed: 11578905]

42. O'Neill B, Magnolato D, Semenza G. The electrogenic, Na^+-dependent I^- transport system in plasma membrane vesicles from thyroid glands. *Biochim Biophys Acta* 896: 263–274, 1987. [PubMed: 3801472]

43. Pastan I Absorption and secretion of iodide by the intestine of the rat. *Endocrinology* 61: 93–97, 1957. [PubMed: 13437959]

44. Perron B, Rodriguez AM, Leblanc G, Pourcher T. Cloning of the mouse sodium iodide symporter and its expression in the mammary gland and other tissues. *J Endocrinol* 170: 185–196, 2001. [PubMed: 11431151]

45. Quaroni A, Wands J, Trelstad RL, Isselbacher KJ. Epithelioid cell cultures from rat small intestine. Characterization by morphologic and immunologic criteria. *J Cell Biol* 80: 248–265, 1979. [PMCID: PMC2110349] [PubMed: 88453]

46. Riedel C, Levy O, Carrasco N. Post-transcriptional regulation of the sodium/iodide symporter by thyrotropin. *J Biol Chem* 276: 21458–21463, 2001. [PubMed: 11290744]

47. Spitzweg C, Joba W, Eisenmenger W, Heufelder AE. Analysis of human sodium iodide symporter gene expression in extrathyroidal tissues and cloning of its complementary deoxyribonucleic acids from salivary gland, mammary gland, and gastric mucosa. *J Clin Endocrinol Metab* 83: 1746–1751, 1998. [PubMed: 9589686]

48. Tazebay UH, Wapnir IL, Levy O, Dohan O, Zuckier LS, Zhao QH, Deng HF, Amenta PS, Fineberg S, Pestell RG, Carrasco N. The mammary gland iodide transporter is expressed during lactation and in breast cancer. *Nat Med* 6: 871–878, 2000. [PubMed: 10932223]

49. Vassart G, Dumont JE. The thyrotropin receptor and the regulation of thyrocyte function and growth. *Endocr Rev* 13: 596–611, 1992. [PubMed: 1425489]

50. Vayre L, Sabourin JC, Caillou B, Ducreux M, Schlumberger M, Bidart JM. Immunohistochemical analysis of Na^+/I^- symporter distribution in human extra-thyroidal tissues. *Eur J Endocrinol* 141: 382–386, 1999. [PubMed: 10526253]

51. Wapnir IL, Goris M, Yudd A, Dohan O, Adelman D, Nowels K, Carrasco N. The Na^+/I^- symporter mediates iodide uptake in breast cancer metastases and can be selectively down-regulated in the thyroid. *Clin Cancer Res* 10: 4294–4302, 2004. [PubMed: 15240514]

52. Wapnir IL, van de Rijn M, Nowels K, Amenta PS, Walton K, Montgomery K, Greco RS, Dohan O, Carrasco N. Immunohistochemical profile of the sodium/iodide symporter in thyroid, breast, and other carcinomas using high density tissue microarrays and conventional sections. *J Clin Endocrinol Metab* 88: 1880–1888, 2003. [PubMed: 12679487]

53. Weiser MM Intestinal epithelial cell surface membrane glycoprotein synthesis. I. An indicator of cellular differentiation. *J Biol Chem* 248: 2536–2541, 1973. [PubMed: 4698230]

54. Weiss SJ, Philp NJ, Grollman EF. Iodide transport in a continuous line of cultured cells from rat thyroid. *Endocrinology* 114: 1090–1098, 1984. [PubMed: 6705729]

55. Wolff J Transport of iodide and other anions in the thyroid gland. *Physiol Rev* 44: 45–90, 1964. [PubMed: 14105583]

Figures and Tables

Fig. 1.

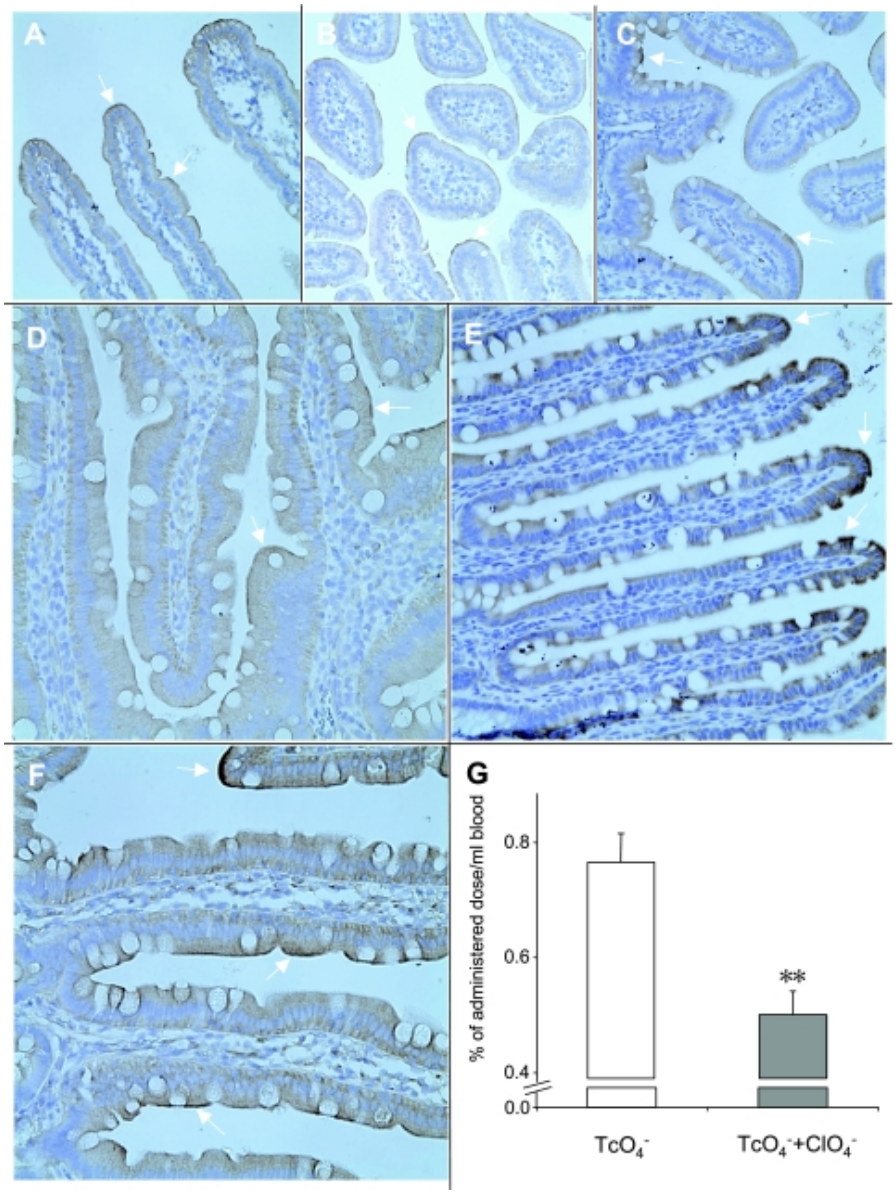

Functional expression of Na^+/I^- symporter (NIS) in mouse and rat small intestine. Small intestine was harvested and immunohistochemistry was carried out with 6.7 nM anti-NIS antibody as described in MATERIALS AND METHODS. In all investigated sections, which included the entire small intestine of each animal, NIS-specific staining was visible in the apical membrane of the epithelial layer (arrows). Mouse (*A*, duodenum; *B*, jejunum; and *C*, ileum) and rat (*D*, duodenum; *E*, jejunum; and *F*, ileum). Magnification ×40 except in *F* (×100). *G*: NIS mediates intestinal $^{99m}TcO_4^-$ uptake in vivo. $^{99m}TcO_4^-$ alone (open bars) and $^{99m}TcO_4^-$ and $NaClO_4$ (100 to 580 nmol; solid bars) were administered at 2-h intervals to 4 rats via a duodenal catheter, and blood samples were collected as described in MATERIALS AND METHODS. Shown is the 9-min time point. $^{**}P < 0.01$ in unpaired *t*-test.

Fig. 2.

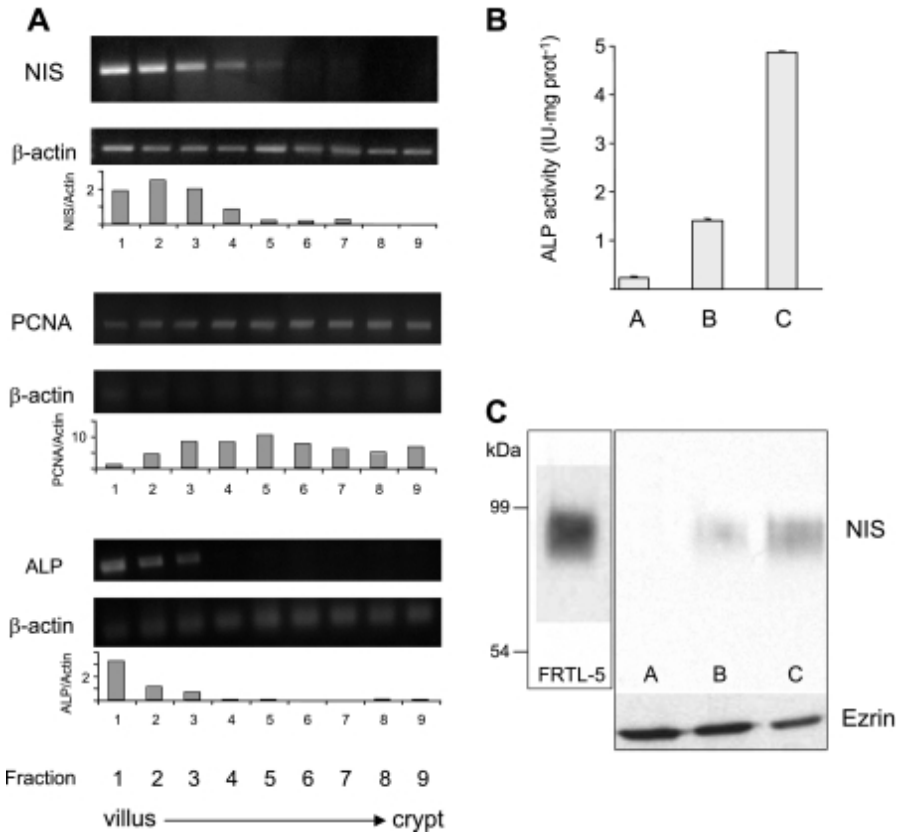

NIS mRNA and protein expression along the villus-crypt axis. *A*: total RNA was extracted from enterocytes sequentially isolated, in nine fractions, from the small intestine along the villus-crypt axis as described in MATERIALS AND METHODS. Differential expression of NIS mRNA was analyzed by RT-PCR and standardized with respect to β-actin mRNA expression. Purity of the villus-crypt fraction separation was confirmed by analysis of the expression of alkaline phosphatase (ALP; a villus marker) and PCNA (a crypt marker) mRNAs. Densitometric ratios of NIS, PCNA, and ALP over β-actin expression are shown. *B*: ALP activity from villus-tip epithelial cells in *fractions A* (homogenate), *B* (nonpurified apical membranes), and *C* (enriched apical membranes). *C*: NIS immunoblot: *lane 1*, FRTL-5 cell membranes (10 μg); *lanes 2-4*, *fraction A*, *B*, or *C* (50 μg). *Bottom*: ezrin immunoblot as loading control after stripping anti-NIS antibodies. Boxes indicate different gels.

Fig. 3.

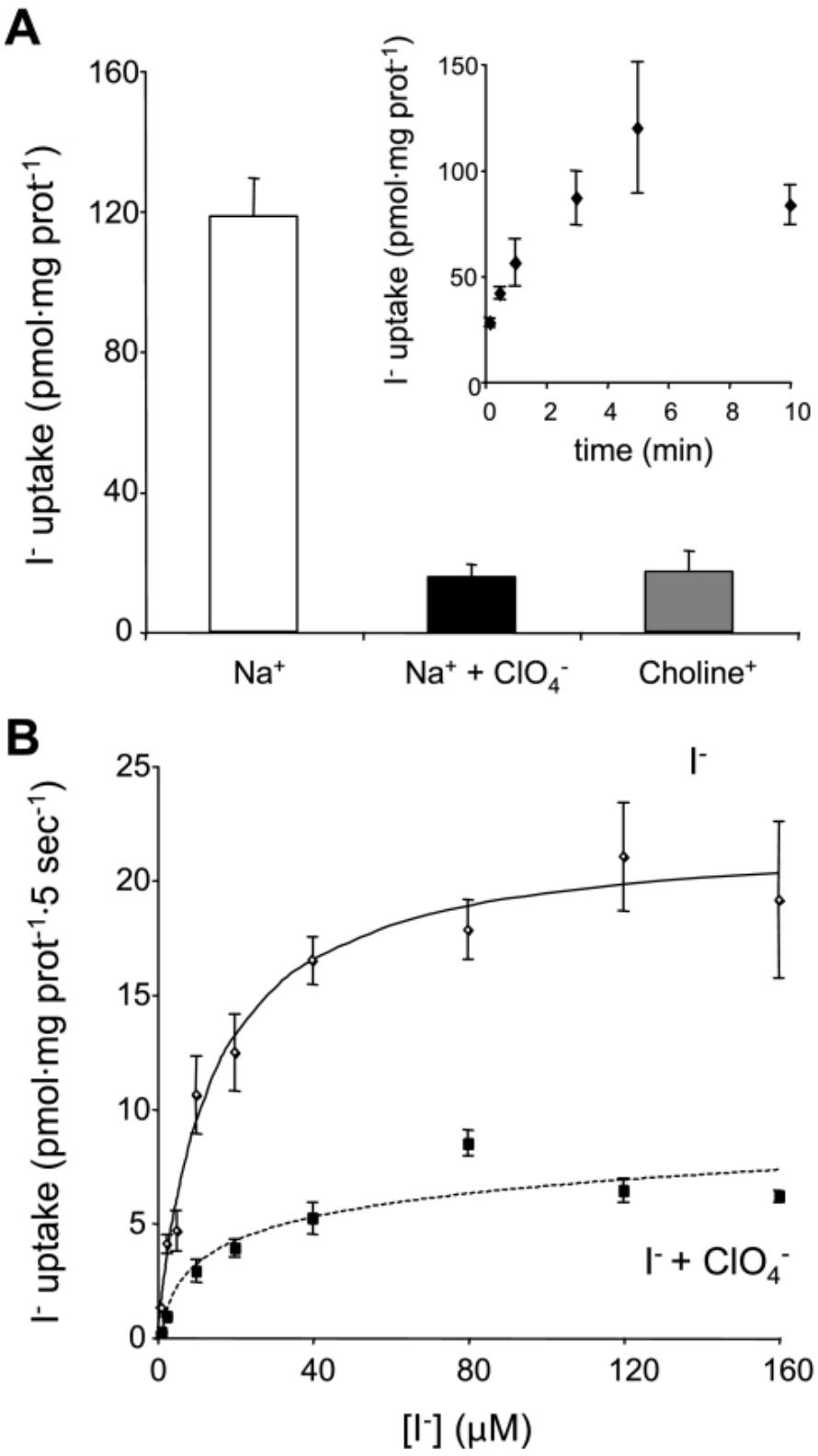

I^- uptake in rat small intestine brush border membrane vesicles (BBMV). *A*: steady-state I^- uptake assays (5-min time points; see *inset* for time course) in BBMV (50 μg) were carried out with 20 μM I^-/140 mM Na^+ (white bar), 20 μM I^-/140 mM Na^+/40 μM ClO_4^- (black bar), and 20 μM I^-/140 mM choline (gray bar) as described in MATERIALS AND METHODS. I^- transport displayed NIS-specific characteristics, i.e., Na^+ dependence and ClO_4^- sensitivity. *Inset*: time course of I^- uptake in BBMV. Transport saturated at 5 min. *B*: initial rates (5-s time points) of I^- uptake were determined at the indicated I^- concentrations and a constant concentration of Na^+ (140 mM) in the absence (solid line) or presence (dotted line) of 40 μM

ClO_4^- as described in MATERIALS AND METHODS. Data were processed using the equation $v = V_{max}[I^-]/[K_m + (I^-)]$. Data were fitted by nonlinear least squares using Gnuplot software. The background, corresponding to time point 0 for each concentration of I^-, was subtracted. Nonspecific I^- binding was 38.4 ± 3.0% of the transport value. NIS exhibited a K_m value for I^- of 13.4 ± 2.0 μM and a V_{max} of 22.0 ± 0.9 pmol I^-/mg protein. All kinetic parameters were determined at least in triplicate and are expressed as means ± SE.

Fig. 4.

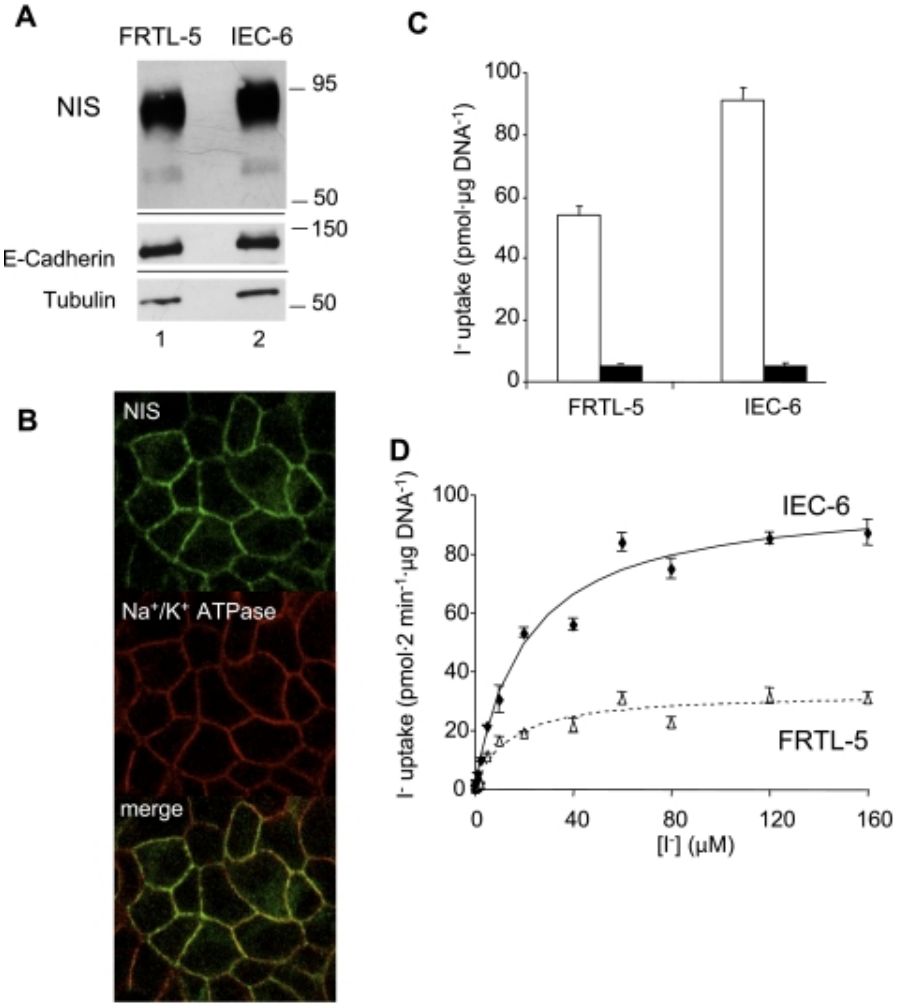

Functional expression of NIS in epithelial cell line 6 (IEC-6) cells. NIS expression was assessed by immunoblot *A*: total protein extracts (10 µg) from FRTL-5 and IEC-6 cells; proteins were electrophoresed and electroblotted as described previously (15) and probed with 2.2 nM polyclonal anti-NIS antibody. *B*: NIS expression in IEC-6 cells analyzed by indirect immunofluorescence. Permeabilized IEC-6 cells were incubated with rabbit anti-NIS antibody (*top*), mouse anti-α_1-subunit of the Na^+-K^+-ATPase antibody (*middle*), and subsequently with Alexa-594-tagged anti-mouse IgG and Alexa-488-tagged anti-rabbit IgG antibodies as described in MATERIALS AND METHODS. Overlay of the two images is shown at *bottom*. NIS is clearly localized at the plasma membrane of IEC-6 cells and colocalized with the Na^+/K^+ ATPase signal. *C*: steady-state (40 min) $^{125}I^-$ transport assay in FRTL-5 and IEC-6 cells performed with 20 µM I^-/140 mM Na^+ (open bars) or 20 µM I^-/140 mM Na^+/80 µM ClO_4^- (solid bars). *D*: initial rates (2-min time points) of NIS-mediated I^- transport in IEC-6 (solid line) or FRTL-5 (dotted line) cells were determined at varying concentrations of I^- and a constant concentration of Na^+ (140 mM). Data were processed using the equation $v = V_{max}[I^-]/[K_m + (I^-)]$. Background values obtained in the presence of ClO_4^- were subtracted. Data were fitted by nonlinear least squares using Gnuplot software. All kinetic parameters were determined at least in triplicate and are expressed as means ± SE.

Fig. 5.

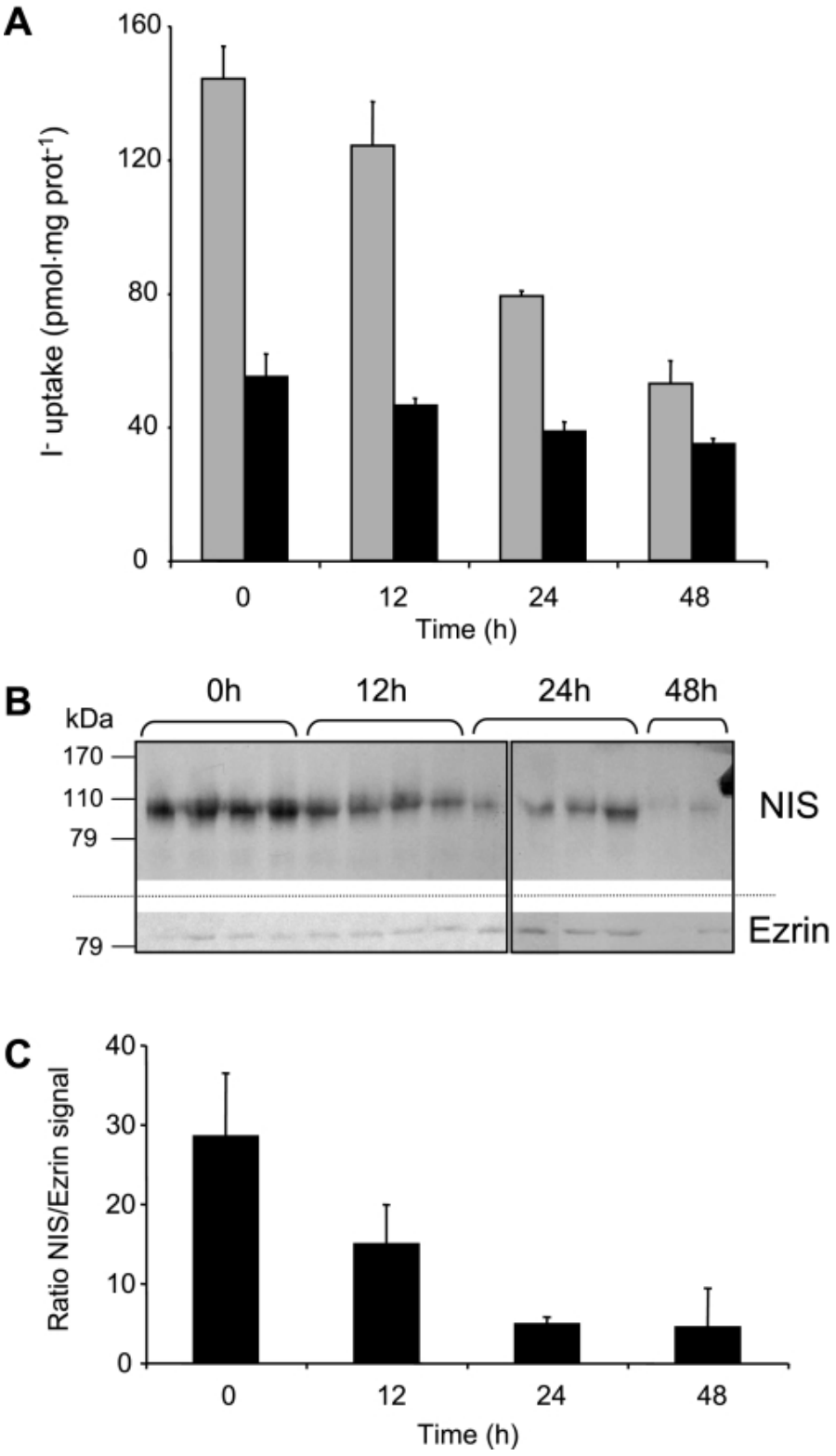

A high-I^- diet reduces intestinal I^- transport and NIS protein in vivo. Rats were provided water (control) or 0.05% KI-supplemented water. After the indicated times, BBMV were purified as described in MATERIALS AND METHODS, and a steady-state I^- uptake assay was performed (*A*) with 50 μg protein and 20 μM $^{125}I^-$ alone (gray bars) or in the presence of 80 μM ClO_4^- (dark bars). *B*: BBMV (100 μg) were also used for immunoblot and probed with anti-NIS and, after stripping the nitro-

cellulose, anti-ezrin antibodies. Ezrin was probed as a loading control, as described in MATERIALS AND METHODS. Boxes indicate different gels. *C*: quantitation of the NIS/ezrin densitometric signal was done with ImageJ software (National Institutes of Health, Bethesda, MD).